Hindawi
International Journal of Photoenergy
Volume 2023, Article ID 7208502, 11 pages
https://doi.org/10.1155/2023/7208502

Research Article

Numerical Simulation of High Efficiency Environment Friendly $CuBi_2O_4$-Based Thin-Film Solar Cell Using SCAPS-1D

Kushal Sarker, Md. Shamsujjoha Sumon, Mst. Farzana Orthe, Sunirmal Kumar Biswas, and Md. Mostak Ahmed

Department of Electrical and Electronic Engineering, Prime University, 114/116 Mazar Road, Dhaka, Bangladesh

Correspondence should be addressed to Kushal Sarker; pu50eee1126@primeuniversity.edu.bd

Received 23 December 2022; Revised 10 March 2023; Accepted 31 March 2023; Published 26 April 2023

Academic Editor: Qiliang Wang

In this research work, a copper bismuth oxide- ($CuBi_2O_4$-) based thin-film solar cell has been proposed for the lead and toxic-free (Al/ITO/TiO_2/$CuBi_2O_4$/Mo) structure simulated in SCAPS-1D software. The main aim of this work to make an ecofriendly and highly efficient thin-film solar cell. The absorber layer $CuBi_2O_4$, buffer layer TiO_2, and the electron transport layer (ETL) ITO have been used in this simulation. The performance of the suggested photovoltaic devices was quantitatively evaluated using variations in thickness such as absorber, buffer, defect density, operating temperature, back contact work function, series, shunt resistances, acceptor density, and donor density. The absorber layer thickness is fixed at 2.0 μm, the buffer layer at 0.05 μm, and the electron transport layer at 0.23 μm, respectively. The $CuBi_2O_4$ absorber layer produces a solar cell efficiency of 31.21%, an open-circuit voltage (V_{oc}) of 1.36 V, short-circuit current density (J_{sc}) of 25.81 mA/cm^2, and a fill factor (FF) of 88.77%, respectively. It is recommended that the proposed $CuBi_2O_4$-based structure can be used as a potential for thin-film solar cells that are both inexpensive and highly efficient.

1. Introduction

The rising depletion of fossil fuels and their detrimental influence on the environment create concerns about the improvement of clean and renewable energy supplies [1–3]. Solar energy is a practical alternative energy source given the declining use of fossil fuels. Due to their comparatively cheap production costs, high absorption coefficient, low surface recombination rates, and comparatively high efficiency, thin-film solar cells witnessed a major boost in their power conversion efficiency (PCE) a little over ten years ago [4, 5]. A thin-film solar cell is a second-generation solar cell that is made by depositing one or more thin layers, or thin film (TF) of photovoltaic material on a substrate, such as glass, plastic, or metal. Thin-film solar cells are commercially used in several technologies, including cadmium telluride (CdTe), copper indium gallium diselenide (CIGS), and amorphous thin-film silicon (a-Si, TF-Si) [6–8]. On the other hand, cadmium (Cd) has frequently been used as an absorber layer material [9–12]. But it is also unfit for the environment. To overcome these drawbacks, a $CuBi_2O_4$-based thin-film solar cell has been proposed in this study. $CuBi_2O_4$ is used as an absorber layer material in a few studies with traditional efficiencies. Another reason for selecting this structure is that it is environmentally friendly. Bismuth ($CuBi_2O_4$) metal has low toxicity to humans and poses minimum threat to the environment. Bismuth compounds generally have very low solubility, but they should be handled with care, as there is only limited information on their effects and fate in the environment [13]. Copper-based ternary oxide semiconductors with tiny energy bandgaps have lately drawn a lot of attention as a photocathode material for solar energy conversion [14]. In Cu, a chemical element with the atomic number 29, group 11, period 4, and a very high thermal and electrical conductivity, is present in $CuBi_2O_4$ materials [15]. The absorber layer $CuBi_2O_4$ is one of the most promising photocathode materials for solar cell technology because of its low cost and ease of manufacturing [14, 16, 17]. The $CuBi_2O_4$ possesses properties that are close to the optimal standard for solar cell application nontoxicity and abundant resource [18–20]. One benefit of $CuBi_2O_4$ is its tiny energy bandgap,

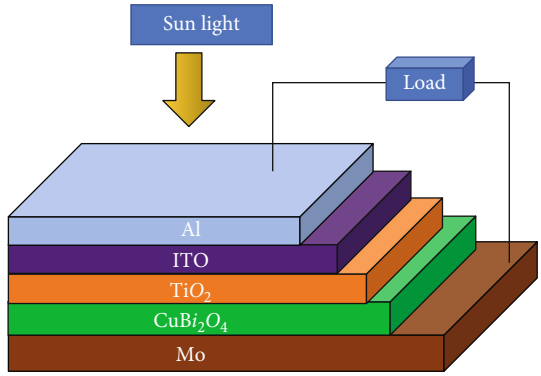

Figure 1: Schematic diagram of proposed (Al/ITO/TiO_2/$CuBi_2O_4$/Mo) thin-film solar cell.

which varies from 1.4 to 1.8 eV. Previous $CuBi_2O_4$-based work structures Al/FTO/CdS/$CuBi_2O_4$/Ni, ITO/SnS/CBO/Au, and ITO/WS_2/CBO/Au are fabricated by SCAPS-1D software. Their efficiencies are 22.84%, 26%, and 27.73%, respectively [21]. In this study, the structure Al/ITO/TiO_2/$CuBi_2O_4$/Mo is designed for the first time, and we obtain the efficiency 31.2%. TiO_2 is used as the buffer layer. Titanium dioxide (TiO_2), a wide-bandgap semiconductor with a high refractive index, has a tremendous potential for use in electronics and optoelectronics. This is because of its transparency in the visible spectral range. TiO_2 is renowned for its wide range of applications and bandgap of more than 3 eV. However, the pure bandgap of TiO_2 is 3.2 eV. Titanium dioxide (TiO_2) is a natural oxide of the element titanium with low toxicity and negligible biological effects. This is why TiO_2 is used here instead of CdS [22]. Several hole-transport layer (HTL) materials with a thin-film absorber layer were used in earlier investigations. In addition to improve the performance of the solar cell, HTL is free in this structure. Eliminating the hole-transport layer (HTL) in this solar cell structure avoids oxidation, reduces costs, and provides better stability and more consistent results [23]. ETL plays an important role in thin-film solar cell. Hence, an appropriate selection of good ETL material for getting an efficient thin film is the need of the hour. Several ETL materials like ZnO, ITO, and CdS were tried to improve the efficiency [24–26]. In this case, ITO acts as an electron transport layer, because we got the maximum efficiency in ITO. The materials for the front and back contacts are aluminum and molybdenum, respectively. By using SCAPS-1D, we investigate the performance parameters such as open-circuit voltage (V_{oc}), short-circuit current (J_{sc}), fill factor (FF), and the efficiency (η). The effects of temperature, series and shunt resistances, energy bandgap, defect density, and the ETL (absorber layer, buffer layer) thickness on device performance are discussed in this paper. The creation of non-toxic, ecofriendly thin-film solar cells in suitable places may benefit from these investigations.

2. Device Architecture and Simulation

Figure 1 shows the Al/ITO/TiO_2/$CuBi_2O_4$/Mo structural characterization of the device which is created and simulated using the SCAPS-1D software program. In the proposed structure, TiO_2 was used as buffer layer, and ITO was used as ETL in $CuBi_2O_4$-based solar cell. Table 1 shows the required parameters for the simulation.

Table 1: Required parameters for the simulation of ITO/TiO_2/$CuBi_2O_4$ (CB = conduction band; VB = valence band).

Parameters (unit)	ITO (ETL) [31]	TiO_2 (buffer) [19]	$CuBi_2O_4$ (absorber) [14]
Thickness (μm)	0.23	0.05	2
Bandgap (eV)	3.6	3.2	1.5
Electron affinity (eV)	4.1	4.2	3.72
Dielectric permittivity (relative)	10	10	34
CB effective DOS (cm^{-3})	$2.2E+18$	$2E+17$	$1.2E+19$
VB effective DOS (cm^{-3})	$1.8E+19$	$6E+17$	$5E+19$
Electron thermal velocity (cm/s)	$1E+7$	$1E+7$	$1E+7$
Hole thermal velocity (cm/s)	$1E+7$	$1E+7$	$1E+7$
Electron mobility (cm^2/V-s)	$1E+2$	$1E+2$	$1.1E-3$
Hole mobility (cm^2/V-s)	$2.5E+1$	$2.5E+2$	$1.2E-3$
Donor density N_D (cm^{-3})	$1E+5$	$1E+17$	0
Acceptor density N_A (cm^{-3})	0	0	$1.7E+18$

At the Department of Electronics and Information Systems (EIS) of the University of Gent in Belgium, a program named SCAPS-1D for "Solar Cell Capacitance Simulator One-Dimensional" was developed to simulate solar cells [27, 28].

Poisson's equation and the continuity equation for the free electrons and holes in the conduction and valence bands are given. The continuity equations for electrons and holes are

$$\frac{d_{Jn}}{dx} = G - R,$$
$$\frac{d_{Jp}}{dx} = G - R, \quad (1)$$

where J_n and J_p are electron and hole current densities, R is the recombination rate, and G is the generation rate.

The Poisson equation is

$$\frac{d^2}{dx^2}\psi(x) = \frac{e}{\varepsilon o\, \epsilon r}\left(\rho(x) - n(x) + N_D - N_A + \rho_p - \rho_n\right), \quad (2)$$

where ψ is the electrostatic potential, e is the electrical charge, ε_r is the relative and ε_0 is the vacuum permittivity, p and n are hole and electron concentrations, N_D is charged impurities of donor, N_A is the acceptor type, and ρ_p and ρ_n are hole and electron distributions, respectively [29, 30].

The SCAPS-1D program was used to extract the energy band diagram for the suggested Al/ITO/TiO2/

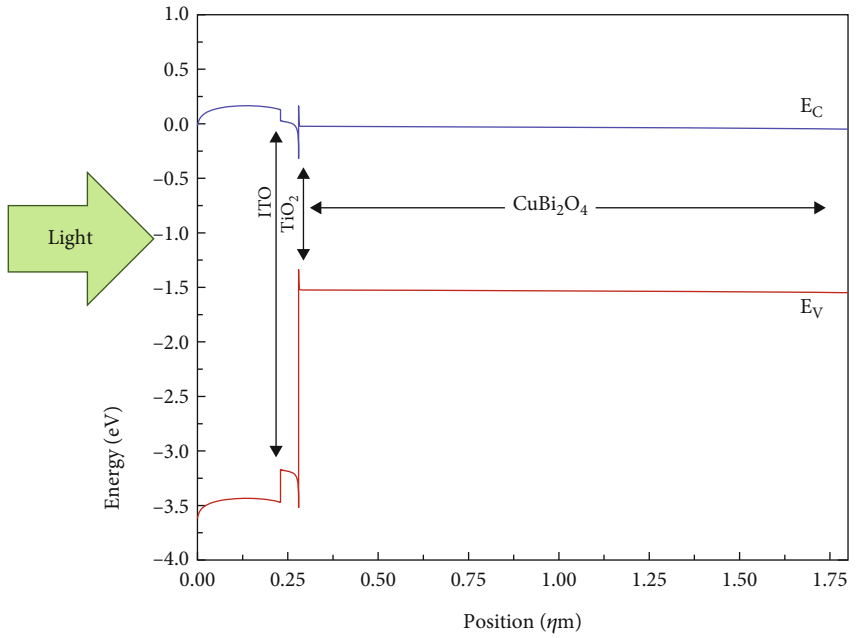

Figure 2: Energy band diagram of $CuBi_2O_4$-based solar cell.

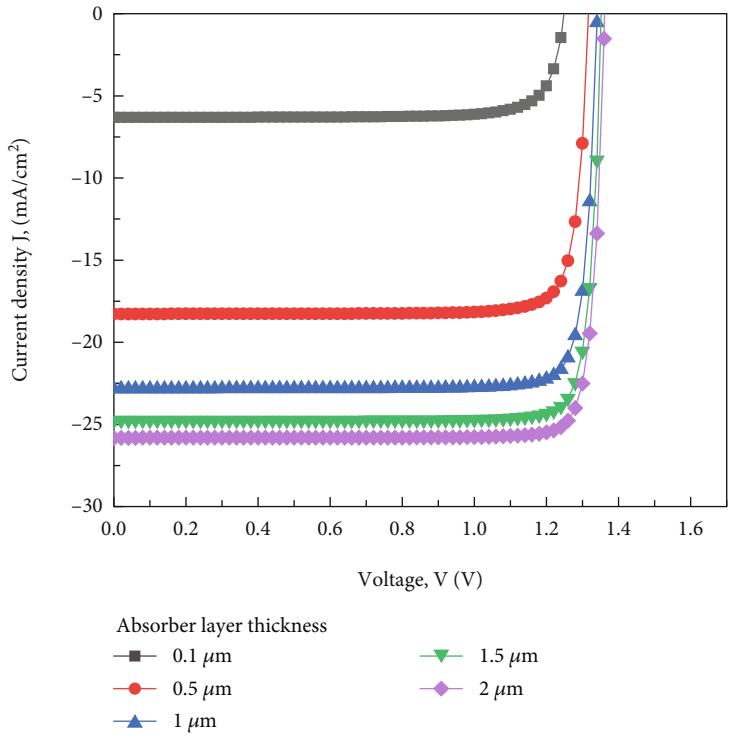

Figure 3: J-V characteristics of the proposed thin-film solar cell by varying.

$CuBi_2O_4$/Mo thin-film solar cell. The optical characteristics of solar cells are discussed using the energy band diagram (Figure 2).

3. Result and Discussions

3.1. J-V Characteristics. By varying the $CuBi_2O_4$ thickness of the absorber layer, Figure 3 demonstrates the J-V characteristics. The buffer layer and ETL settings are fixed, whereas the absorber layer's thickness varies here from 0.1 to 2 μm, and current and voltage rise with an increasing efficiency of 6.4% to 31.21%. From the J-V curve, it can be found that efficiency increases continuously as absorber thickness increases. Increased current and voltage are caused by the addition of the electron-hole pair during the thickness of the absorber layer.

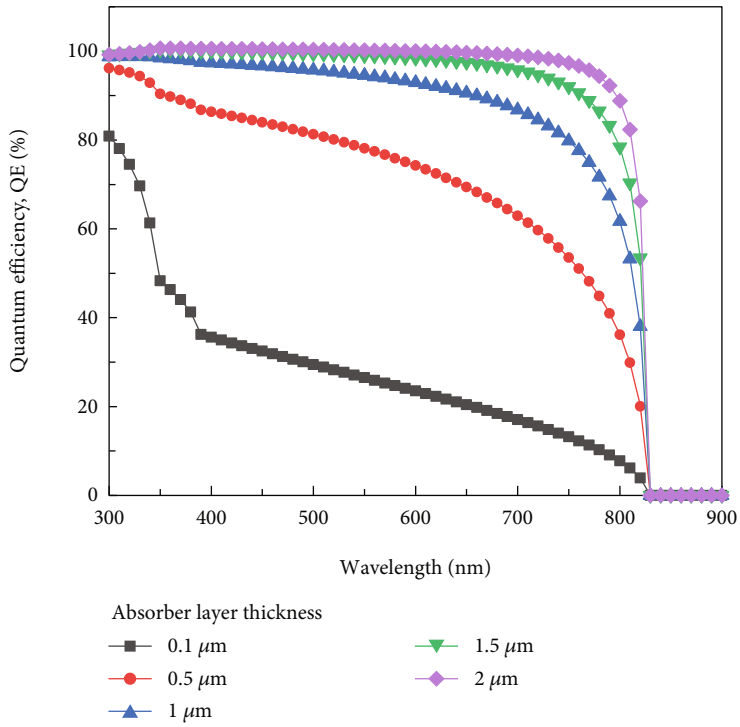

Figure 4: Quantum efficiency vs. wavelength for various absorber thicknesses.

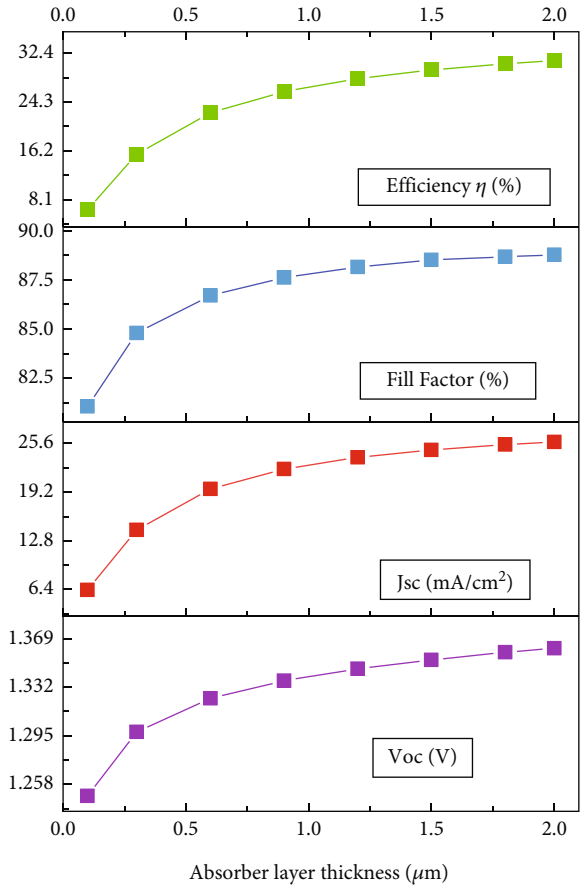

Figure 5: Effect of absorber layer thickness on output parameters such as V_{oc}, J_{sc}, FF, and efficiency.

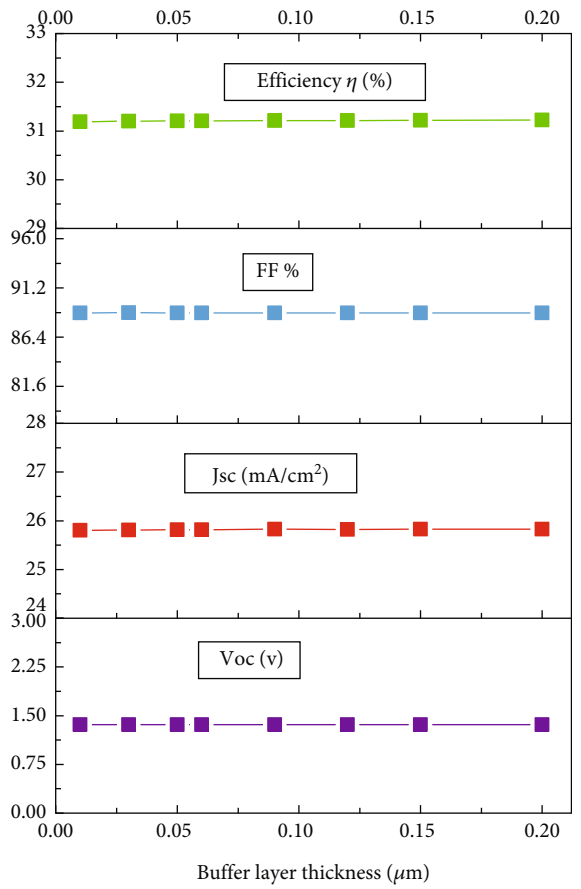

Figure 6: Effect of buffer layer thickness on output parameters such as V_{oc}, J_{sc}, FF, and efficiency.

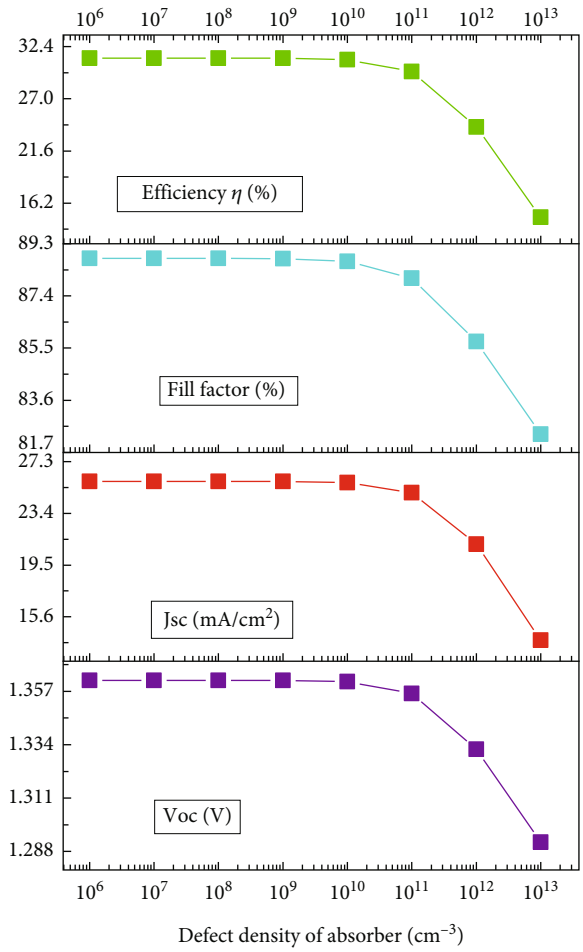

Figure 7: Effect of defect density in the absorber layer on PV performance with respect to V_{oc}, J_{sc}, FF, and efficiency.

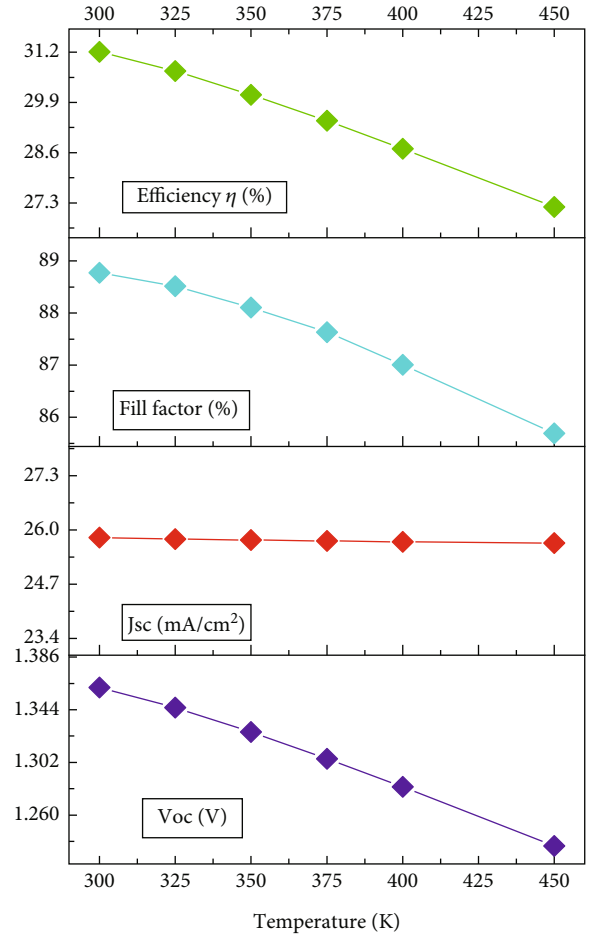

Figure 8: Effect of operating temperature on PV parameters such as V_{oc}, J_{sc}, FF, and efficiency.

3.2. Quantum Efficiency. The ratio of carriers collected by the solar cell to photon incident on the solar cell at a specific energy is here described as the quantum efficiency. It might also be stated as a function of wavelength or as an energy value [32]. In Figure 4, the QE rises at longer wavelengths as the absorber layer thickness increases. This is because there are less electron-hole pairs produced by photons inside the absorber layer. Additionally, for longer wavelengths of low energy, light is not absorbed below bandgaps, which causes quantum efficiency to drop to zero for wavelengths greater than 810 nm. The $CuBi_2O_4$ absorber layer's thickness changed from 0.1 to 2.0 μm, and the ITO and TiO_2 layers' thicknesses were fixed at 0.23 μm and 0.05 μm, respectively.

3.3. Effect of Variation in Absorber Layer Thickness. The thickness of the active layer is one of the most important parameters in increasing the performance of solar cells [33, 34]. The models were simulated at various absorber layer thicknesses, and then, a regression analysis model was made to determine the efficiency and fill factor at each specified value. According to Figure 5, the fill factor, current density, and open-circuit voltage of this arrangement rise as the thickness of the absorber layer increases. When the absorber layer thickness is 0.1 μm, the values of the efficiency, V_{oc}, J_{sc}, and FF are 6.4%, 1.24 V, 6.32 mA/cm^2, and 81.06%, respectively. When absorber layer thickness is 2.0 μm, the values of the efficiency, V_{oc}, J_{sc}, and FF are 31.2%, 1.36 V, 25.81 mA/cm^2, and 88.76%, respectively. This might be accounted for by the fact that as the $CuBi_2O_4$ layer becomes thicker, more short-wavelength photons are absorbed, which promotes the photogeneration of additional free carriers [35].

3.4. Effect of the Buffer Layer Thickness. The impact of TiO_2 thickness on $CuBi_2O_4$-based solar cells is displayed in Figure 6. Here, the absorber layer thickness was fixed at 2 μm while the TiO_2 thickness was increased from 0.01 μm to 0.2 μm. Here, when the thickness is 0.01 μm, in that time, the efficiency is 31.18%, V_{oc}1.36 V, J_{sc}25.8 mA/cm^2, and the fill factor 88.76%, and when the thickness is 0.2 μm, then the efficiency is 31.21%, V_{oc}1.36 V,J_{sc}25.82 mA/cm^2, and the fill factor 88.76%. It is seen that all the parameters are stable for all the points. It is because fewer photons will reach the absorber through the thicker buffer layer [36–38].

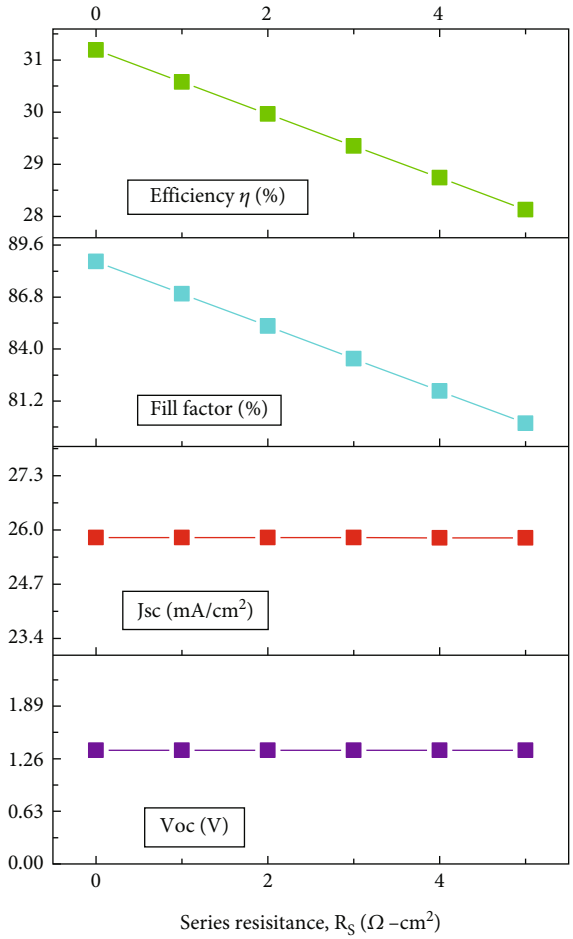

Figure 9: Effect of series resistance with respect to V_{oc}, J_{sc}, FF, and efficiency.

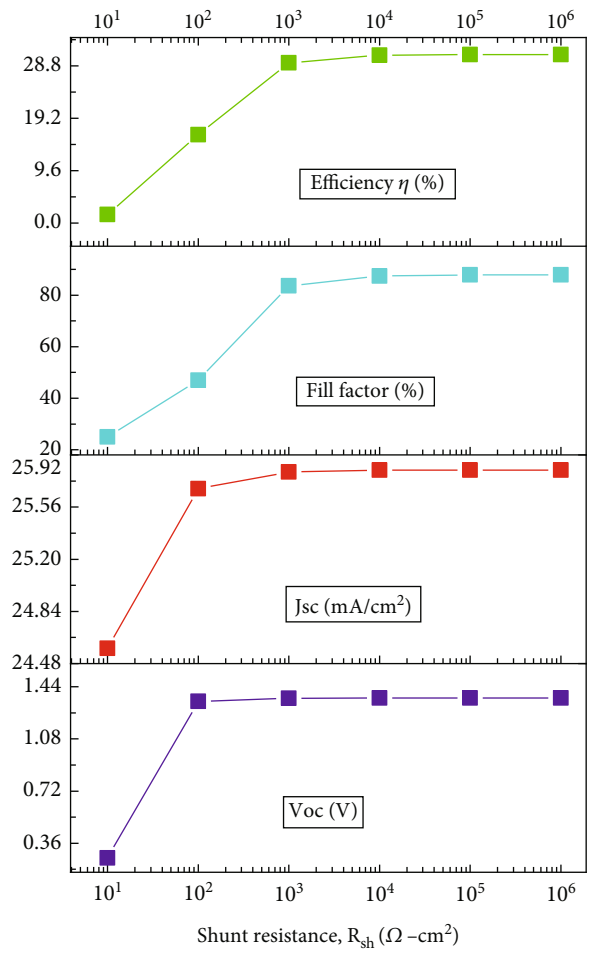

Figure 10: Effect of shunt resistance with respect to V_{oc}, J_{sc}, FF, and efficiency.

3.5. Effect of Defect Density on the Absorber Layer. The defect density in the absorber layer was changing from 10^6 to 10^{13} cm^{-3} while holding other parameters fixed (Figure 7). All cell parameters are significantly impacted by the absorber defect; when the defect density is 10^6 cm^{-3}, the values of the efficiency, V_{oc}, J_{sc}, and fill factor are 24.07%, 1.36 V, 25.81 mA/cm^2, and 88.76%, respectively. When the defect density is 10^{13}, the values of efficiency, V_{oc}, J_{sc}, and FF are 14.73%, 1.29 V, 13.84 mA/cm^2, and 82.36%, respectively. The open-circuit voltage V_{oc} decreases as the defect concentration increases. The short-circuit current J_{sc} decreases as a result of the carrier recombination [39]. The fill factor (FF), as shown in Figure 7, decreases in a manner similar to that of the external quantum efficiency η (%) [40].

3.6. Effect of Temperature. Operating temperature has a big impact on how well solar cells work [41]. Temperature variations have an effect on the solar cell's overall performance. Efficiency is affected by temperature, as seen in Figure 8. As shown in the figure for both configurations, the working temperature was then varied between 300 K and 450 K to assess its effects on PCE, V_{oc}, J_{sc}, and FF for the ideal absorber thickness. When the temperature is at 300 K, the values of the efficiency, V_{oc}, and FF are 31.2%, 1.36 V, and 88.76%, respectively. When the temperature is at 450 K, the values of the efficiency, V_{oc}, and FF are 27.19%, 1.23 V, and 85.69%, respectively. J_{sc} is stable here. It is observed that by increasing working temperature, the efficiency was decreasing. The velocity of charged particles increases as temperature rises [42]. The rate of electron and hole recombination rises as temperature rises because there are fewer free electrons and holes available [43].

3.7. Effects of Series and Shunt Resistances. The performance of a device is greatly influenced by the series and shunt resistances. Efficiency changed in this example due to the effect of changing series resistance. Keeping R_{sh} set at 10^5Ω-cm^2, the series resistance performance is explored by changing R_S 0 to 5 Ω-cm^2. As series resistance rises, the efficiency decreased. The initial efficiency was 31.2%. At the final resistance, the efficiency was 28.1%, FF was 80%, and V_{oc} and J_{sc} were flat by varying the resistance. The series and shunt resistances of a solar cell should be zero and infinite, but in practice, things operate quite differently.

Solar cells' parasitic components and series and shunt resistances exhibit losses. Since recombination in defect

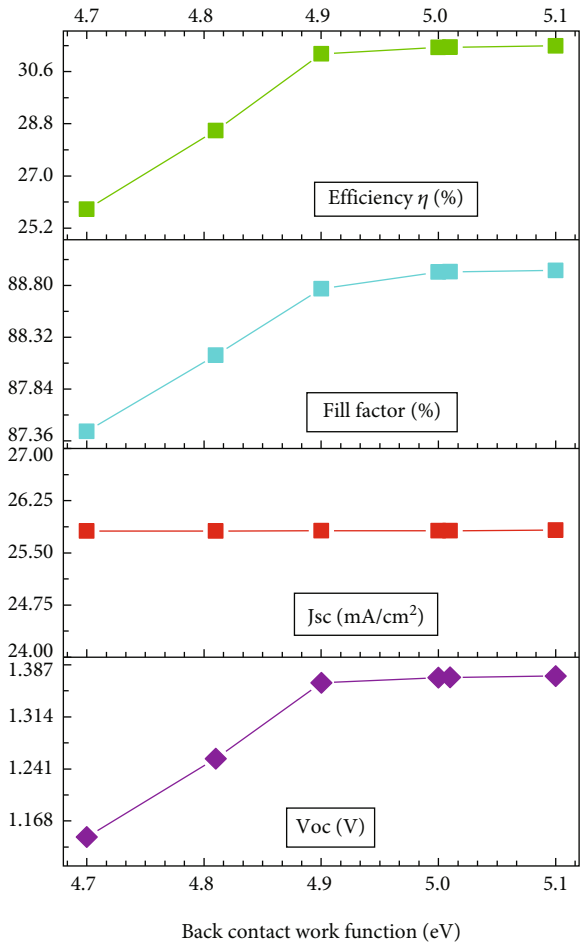

Figure 11: Effect of variation on back contact work function with respect to V_{oc}, J_{sc}, FF, and efficiency.

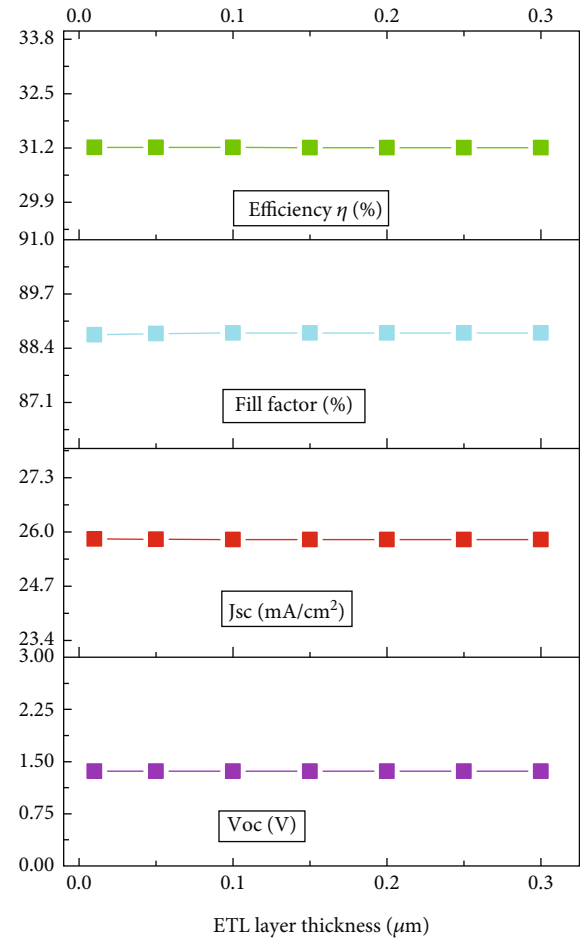

Figure 12: Effect of the ETL thickness variation with respect to V_{oc}, J_{sc}, FF, and efficiency.

states is the primary cause of shunt resistance, the defect state reduces as the device's shunt resistance increases [44]. Series resistance lowers the PV properties of the photovoltaic cell. Figure 9 illustrates the effect of series resistance when the shunt resistance is set at $10^5\Omega$-cm^2 and the series resistance is changed. Figure 10 illustrates the outcome of shunt resistance. The shunt resistance performance is explored by changing R_{sh} from 10^1 to $10^6\Omega$ cm^2, and R_s remains constant at 0.5 Ω cm^2. When R_{sh} is $10^1\Omega$-cm^2, its efficiency increases 1.58% to 30.89% when R_{sh} increases to a higher value. FF, J_{sc}, and V_{oc} are observed at 24.96%, 24.58 mA/cm^2, and 0.25 V, and when R_{sh} is $10^6\Omega$-cm^2, these output parameters varied to 87.88%, 25.81 mA/cm^2, and 1.36 V.

3.8. Effects of Back Contact Work Function. The changing of back contact material work function (eV) and its influence of the parameters are present here. Figure 11 shows the influence of back contact work function on solar cell performance parameters. The electric field of the depletion area produces and separates carriers, which must be collected at metal contacts to power the load. Imperfections in the metal-semiconductor interface will affect the efficiency of solar cells if they are recombined [45–47]. Solar cell efficiency will be aided by the surface field produced by this strongly doped back end. Materials used as back contact include copper, carbon, molybdenum, beryllium, nickel, and gold, with work functions ranging from 4.7 to 5.1. When the work function is 4.7, then the efficiency is 25.85%, V_{oc} 1.14 V, J_{sc} 25.81 mA/cm^2, and FF 87.44%, and when the work function is 5.1, then the efficiency is 31.48%, V_{oc} 1.37 V, J_{sc} 25.82 mA/cm^2, and FF 88.93%. The proposed solar cell structure with metal back contact gold (Au) got the PCE of 31.51% and with molybdenum (Mo) got PCE of 31.21%. The efficiency was not so high with gold (Au) as compared to molybdenum (Mo) as metal back contact, and gold is expensive than molybdenum; that is why we did not use gold (Au) as metal back contact layer with our structure. The efficiency of solar cells will be impacted over the long run if they are recombined as a result of flaws in the metal-semiconductor interface [45].

3.9. Effects of Variations in ETL Thickness. The behavior of the proposed solar cell is also investigated on the basis of altering the ETL thickness. The effect of variations in ETL thickness on performance indicators including V_{oc}, J_{sc}, FF, and conversion efficiency is shown in Figure 12. ETL might range in thickness between 0.1 and 0.5 μm. While the ETL thickness was altered, the thickness of the absorber and

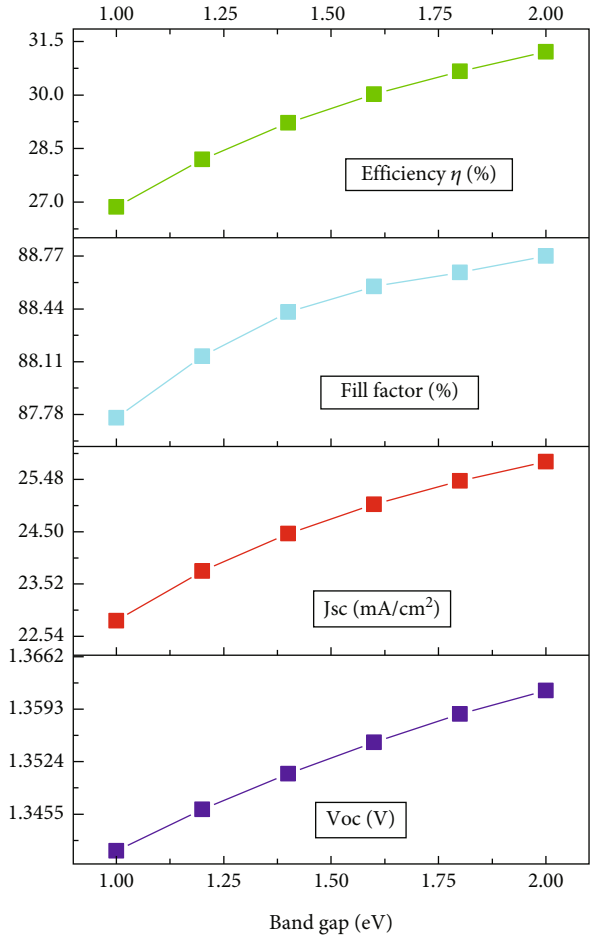

Figure 13: Effect of bandgap variation with respect to V_{oc}, J_{sc}, FF, and efficiency.

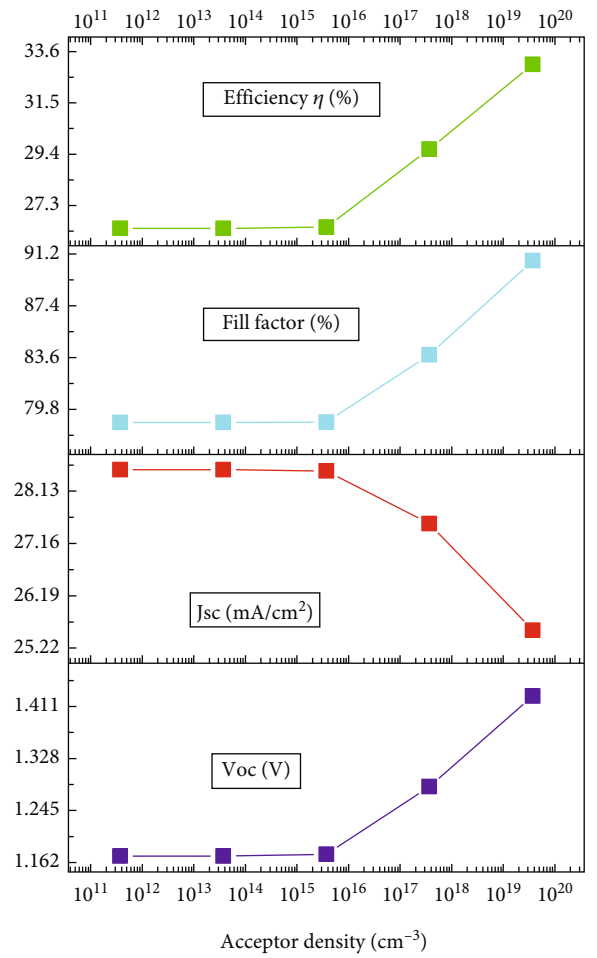

Figure 14: Effect of acceptor density with respect to V_{oc}, J_{sc}, FF, and efficiency.

buffer remained unchanged. The parameters of the solar cell are influenced by the electron transport layer because of ITO's significant defect of intrinsic low mobility [48]. Charge accumulation and ultimately recombination will develop as the layer's thickness does [49].

3.10. Effects of Variations in Bandgap. Numerous factors affect the efficiency and performance of PV cell layouts. A complex internal physical process that occurred is what caused the issue. The performance of PV cell designs must be taken into consideration in a solar cell model. The cause is a complicated internal physical mechanism that has taken place. To trust a solar cell model, we must consider a number of factors as well as many situations that can be tested and compared [50]. We have considered the impact of this on the $CuBi_2O_4$ absorber layer's bandgap. Figure 13 illustrates the effects of bandgap changes. We altered the bandgap from 1 to 2 eV. When the bandgap is 1 eV, the efficiency is 26.8%, V_{oc} 1.34 V, J_{sc} 22.83 mA/cm^2, and FF 87.75%. When the bandgap is 1.6 eV, then the efficiency is 30%, and when the bandgap is 2 eV, the desired efficiency is 31.2%, V_{oc} 1.36 V, J_{sc} 25.81 mA/cm^2, and FF 88.76%. All the parameters increased with the increase of bandgap.

3.11. Effects of Acceptor Density. Figure 14 demonstrates how open-circuit voltage V_{oc} increases and short-circuit current J_{sc} decreases when $CuBi_2O_4$'s acceptor density varies. The fill factor (FF) increases once the acceptor density surpasses 10^{16} cm^{-3} and then slightly rises. The power conversion efficiency (PCE) increased as a result. We also investigated how acceptor density and photovoltaic efficiency are related. Here, when the acceptor density is 3.7×10^{11} cm^{-3}, then the efficiency is 36.36%, V_{oc} 1.72 V, J_{sc} 28.52 mA/cm^2, and FF 78.84%, and when the density is 3.7×10^{19}cm^{-3}, then the efficiency is 33.07%, V_{oc} 1.42 V, J_{sc} 25.54 mA/cm^2, and FF 90.70%. When the photogenerated minority carriers reach the depletion zone of the combination, an existing electrical field separates them [51]. Lower acceptor density would increase the device's series resistance, while higher acceptor density would decrease the device's shunt resistance, thus reducing the performance of the solar cell.

3.12. Effects of Donor Density on the Buffer Layer. Figure 15 shows that the solar cell output parameters V_{oc}, J_{sc}, FF, and η are nearly constant as a function of the thickness of the TiO_2 buffer layer due to the insufficient number of electron-hole pairs produced in the $CuBi_2O_4$ absorber layer.

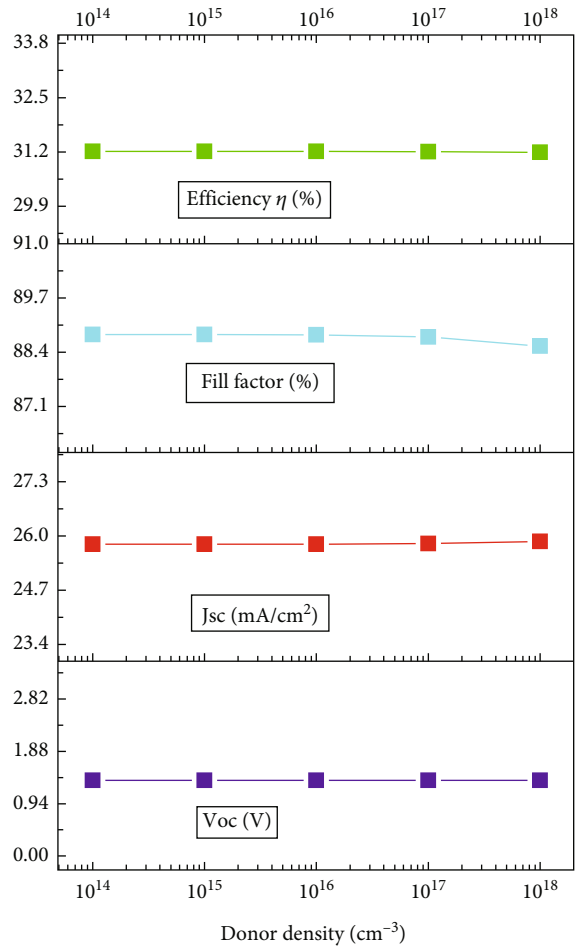

Figure 15: Effect of donor density with respect to V_{oc}, J_{sc}, FF, and efficiency.

Since it is assumed that less light passes through the absorber, because of a thicker buffer layer resulting in a negligible current for insufficient production of photons which creates electrons and holes a thin buffer layer is predicted to give high solar cell activities. In this case, the thickness varied from 10^{14} to 10^{18}.When the donor density is 10^{14} cm^{-3}, then the efficiency is 31.20%, V_{oc} 1.36 V, J_{sc} 25.80 mA/cm^2, and FF 88.82%, and when the density is 10^{18} cm^{-3}, the efficiency is 31.19%, V_{oc} 1.36 V, J_{sc} 25.86 mA/cm^2, and FF 88.54%. Here, graph for the donor density parameters was flat.

4. Conclusion

A numerical investigation of the $CuBi_2O_4$-based thin-film solar cells is carried out using the one-dimensional simulator SCAPS. In this work, SCAPS-1D was used to analyze the optimum nature of $CuBi_2O_4$-based thin-film solar cells with absorber, buffer, defect density, series resistance, shunt resistance, donor, acceptor density, bandgap variation, and ETL topologies. These findings show the creation of HTL free thin-film solar cell made of copper bismuth oxide that is ecologically effective. The defect density in the absorber layer was changing from 10^6 to 10^{13} cm^{-3} and the efficiency was reduced from 24.07% to 14.73%. At a working temperature of 300 K, the best result (31.21%) and an open-circuit voltage of 1.36 V, short-circuit current density of 25.81 mA/cm^2, and a fill factor (FF) of 88.77% were attained. Additionally, it is discovered through research that using suitable back contact materials with a high work function can improve the output performance of the proposed device construction. Mo was used here because of its low cost. Therefore, this simulation study opens a new direction for a simpler, low-cost, highly efficient, and more stable cadmium free $CuBi_2O_4$-based thin-film solar cell.

Data Availability

The data that support the findings of this study are available from the corresponding author upon reasonable request.

Ethical Approval

This research is based on simulation. As a result, during research, this work did not cause any harm to humans, animals, or the environment. The used materials are nontoxic, and we hope this structure will not be harmful for further work.

Conflicts of Interest

There is no conflict of interest.

Acknowledgments

We thankfully acknowledge Dr. Marc Burgelman of the University of Gent in Belgium who has generously provided the SCAPS simulation program.

References

[1] N. Singh, A. Agarwal, and M. Agarwal, "Numerical simulation of highly efficient lead-free all-perovskite tandem solar cell," *Solar Energy*, vol. 208, pp. 399–410, 2020.

[2] W. Ebhota and T.-C. Jen, "Fossil fuels environmental challenges and the role of solar photovoltaic technology advances in fast tracking hybrid renewable energy system," *International Journal of Precision Engineering and Manufacturing-Green Technology*, vol. 7, no. 1, pp. 97–117, 2020.

[3] M. J. B. Kabeyi and O. A. Olanrewaju, "sustainable energy transition for renewable and low carbon grid electricity generation and supply," *Frontiers in Energy Research*, vol. 9, 2022.

[4] S. Srivastava, A. K. Singh, P. Kumar, and B. Pradhan, "Comparative performance analysis of lead-free perovskites solar cells by numerical simulation," *Journal of Applied Physics*, vol. 131, no. 17, article 175001, 2022.

[5] Gagandeep, M. Singh, and R. Kumar, "Simulation of perovskite solar cell with graphene as hole transporting material," in *AIP Conference Proceedings [AIP Publishing DAE SOLID STATE PHYSICS SYMPOSIUM 2018 (18–22 December 2018)]*, Hisar, Haryana, India, 2019.

[6] S. Banerjee, "High efficiency CdTe/CdS thin film solar cell," *International Journal of Engineering Research & Technology*, vol. V4, 2015.

[7] S. Ahmmed, A. Aktar, M. F. Rahman, J. Hossain, and A. B. Ismail, "A numerical simulation of high efficiency CdS/CdTe based solar cell using NiO HTL and ZnO TCO," *Optik*, vol. 223, article 165625, 2020.

[8] M. Samiul Islam, K. Sobayel, A. Al-Kahtani et al., "Defect study and modelling of SnX3-based perovskite solar cells with SCAPS-1D," *Nanomaterials*, vol. 11, no. 5, p. 1218, 2021.

[9] F. A. Jhuma and M. J. Rashid, "Simulation study to find suitable dopants of CdS buffer layer for CZTS solar cell," *Journal of Theoretical and Applied Physics*, vol. 14, no. 1, pp. 75–84, 2020.

[10] J. Qu, L. Zhang, H. Wang, X. Song, Y. Zhang, and H. Yan, "Simulation of double buffer layer on CIGS solar cell with SCAPS software," *Optical and Quantum Electronics*, vol. 51, no. 12, 2019.

[11] M. A. Matin, M. U. Tomal, and A. M. Robin, "Copper telluride as a nobel BSF material for high performance ultra thin CdTe PV cell," in *2013 International Conference on Informatics, Electronics and Vision (ICIEV)*, Dhaka, Bangladesh, 2013.

[12] R. A. Rassol, R. F. Hasan, and S. M. Ahmed, "Numerical analysis of SnO_2/Zn_2SnO_4/n-CdS/p-CdTe solar cell using the SCAPS-1D simulation software," *Iraqi Journal of Science*, vol. 62, pp. 505–516, 2021.

[13] R. Wang, H. Li, and H. Sun, "Bismuth: environmental pollution and health effects," in *Encyclopedia of Environmental Health*, pp. 415–423, Elsevier, 2019.

[14] A. Hosen, M. S. Mian, and S. R. Ahmed, "Simulating the performance of a highly efficient $CuBi_2O_4$-based thin-film solar cell," *SN Applied Sciences*, vol. 3, 2021.

[15] F. Wang, A. Chemseddine, F. F. Abdi, R. van de Krol, and S. P. Berglund, "Spray pyrolysis of $CuBi_2O_4$ photocathodes: improved solution chemistry for highly homogeneous thin films," *Journal of Materials Chemistry A*, vol. 5, no. 25, pp. 12838–12847, 2017.

[16] S. Wei, N. Xu, F. Li et al., "Rationally construct heterojunction on CuBi2O4 photocathode improved activity and stability for photoelectrochemical water reduction," *ChemElectroChem*, vol. 6, no. 13, pp. 3367–3374, 2019.

[17] W. Shi, X. Qiao, J. Wang et al., "Ultra-fast construction of novel S-scheme $CuBi_2O_4$/CuO heterojunction for selectively photocatalytic $CO_{2\ \text{Conversion to CO}}$," *Nanomaterials*, vol. 12, no. 18, p. 3247, 2022.

[18] A. Elaziouti, N. Laouedj, A. Bekka, and R. N. Vannier, "Preparation and characterization of p-n heterojunction $CuBi_2O_4$/CeO_2 and its photocatalytic activities under UVA light irradiation," *Journal of King Saud University-Science*, vol. 27, no. 2, pp. 120–135, 2015.

[19] P. Sawicka-Chudy, Z. Starowicz, G. Wisz et al., "Simulation of TiO_2/CuO solar cells with SCAPS-1D software," *Materials Research Express*, vol. 6, no. 8, article 085918, 2019.

[20] O. Ahmad, A. Rashid, M. W. Ahmed, M. F. Nasir, and I. Qasim, "Performance evaluation of Au/p-CdTe/Cs_2TiI_6/n-TiO_2/ITO solar cell using SCAPS-1D," *Optical Materials*, vol. 117, article 111105, 2021.

[21] Y. K. Reddy, V. Manjunath, S. Bimli, and R. S. Devan, "Futuristic kusachiite solar cells of $CuBi_2O_4$ absorber and metal sulfide buffer layers: theoretical efficiency approaching 28 %," *Solar Energy*, vol. 244, pp. 75–83, 2022.

[22] F. Grande and P. Tucci, "Titanium dioxide nanoparticles: a risk for human health?," *Mini Reviews in Medicinal Chemistry*, vol. 16, no. 9, pp. 762–769, 2016.

[23] S. Li, Y. L. Cao, W. H. Li, and Z. S. Bo, "A brief review of hole transporting materials commonly used in perovskite solar cells," *Rare Metals*, vol. 40, no. 10, pp. 2712–2729, 2021.

[24] M. A. Mahmud, N. K. Elumalai, M. B. Upama et al., "Low temperature processed ZnO thin film as electron transport layer for efficient perovskite solar cells," *Solar Energy Materials and Solar Cells*, vol. 159, pp. 251–264, 2017.

[25] A. Hernández-Granados, A. N. Corpus-Mendoza, P. M. Moreno-Romero et al., "Optically uniform thin films of mesoporous TiO_2 for perovskite solar cell applications," *Optical Materials*, vol. 88, pp. 695–703, 2019.

[26] C. Wessendorf, J. Hanisch, D. Müller, and E. Ahlswede, "CdS as electron transport layer for low-hysteresis perovskite solar cells," *Solar RRL*, vol. 2, no. 5, 2018.

[27] S. Sajid, "Re: How to simulate perovskite solar cell using SCAPS-1D simulation software?," 2021, https://www.researchgate.net/post/How-to-simulate-perovskite-solar-cell-using-SCAPS-1D-simulation-software/609c168e3c02b615a744f44d/citation/download.

[28] J. Verschraegen and M. Burgelman, "Numerical modeling of intra-band tunneling for heterojunction solar cells in SCAPS," *Thin Solid Films*, vol. 515, no. 15, p. 6276, 2007.

[29] H. Movla, "Optimization of the CIGS based thin film solar cells: numerical simulation and analysis," *Optik*, vol. 125, pp. 67–70, 2014.

[30] M. Burgelman, J. Verschraegen, S. Degrave, and P. Nollet, "Modeling thin-film PV devices," *Progress in Photovoltaics: Research and Applications*, vol. 12, pp. 143–153, 2004.

[31] H. T. Ganem and A. N. Saleh, "Enhancement of the efficiency of the CZTS/Cds/Zno/ITO solar cell by back reflection and buffer layers using SCAPS-1D," *Iraqi Journal of Science*, vol. 6, pp. 1144–1157, 2021.

[32] I. T. Bello, D. O. Idisi, K. O. Suleman et al., "Thickness variation effects on the efficiency of simulated hybrid Cu_2ZnSnS_4-based solar cells using SCAPS-1D," *Biointerface Research in Applied Chemistry*, vol. 12, pp. 7478–7487, 2021.

[33] O. O. Shoewu, "Effect of absorber layer thickness and band gap on the performance of CdTe/CdS/ZnO multi-junction thin film solar cell," 2018, https://www.researchgate.net/publication/328410621.

[34] T. Ouslimane, L. Et-Taya, L. Elmaimouni, and A. Benami, "Impact of absorber layer thickness, defect density, and operating temperature on the performance of $MAPbI_3$ solar cells based on ZnO electron transporting material," *Heliyon*, vol. 7, no. 3, article e06379, 2021.

[35] S. Fadili, B. Hartiti, A. Kotbi, A. Ridah, and P. Thevenin, "Numerical simulation of solar cells besed CZTS buffer layer (ZnO1- XSX) using SCAPS-1D software," *Journal of Fundamental and Applied Sciences*, vol. 9, pp. 1001–1011, 2017.

[36] F. Belarbi, W. Rahal, D. Rached, and M. Adnane, "A comparative study of different buffer layers for CZTS solar cell using SCAPS-1D simulation program," *Optik*, vol. 216, article 164743, 2020.

[37] T. Garmim, N. Benaissa, L. Soussi et al., "Effect of alternative buffer layers for SnS based solar cells: numerical analysis using SCAPS-1D," *Materials Today: Proceedings*, vol. 66, pp. 146–150, 2022.

[38] P. Chelvanathan, M. I. Hossain, and N. Amin, "Performance analysis of copper-indium-gallium-diselenide (CIGS) solar cells with various buffer layers by SCAPS," *Current Applied Physics*, vol. 10, no. 3, pp. S387–S391, 2010.

[39] A. S. Chouhan, N. P. Jasti, and S. Avasthi, "Effect of interface defect density on performance of perovskite solar cell: correlation of simulation and experiment," *Materials Letters*, vol. 221, pp. 150–153, 2018.

[40] H. Xie, Z. Wang, Z. Chen et al., "Decoupling the effects of defects on efficiency and stability through phosphonates in stable halide perovskite solar cells," *Joule*, vol. 5, no. 5, pp. 1246–1266, 2021.

[41] A. K. Daoudia, Y. El Hassouani, and A. Benami, "Investigation of the effect of thickness, band gap and temperature on the efficiency of CIGS solar cells through SCAPS-1D," *International Journal of Engineering and Technical Research*, vol. 6, p. 71, 2016.

[42] I. Alam and M. A. Ashraf, "Effect of different device parameters on tin-based perovskite solar cell coupled with In2S3electron transport layer and CuSCN and Spiro-OMeTAD alternative hole transport layers for high-efficiency performance," *Energy Sources, Part A: Recovery, Utilization, and Environmental Effects*, vol. 159, pp. 1–17, 2020.

[43] F. Anwar, S. Afrin, S. S. Satter, R. Mahbub, and S. M. Ullah, "Simulation and performance study of nanowire CdS/CdTe solar cell," *International Journal of Renewable Energy Research*, vol. 7, pp. 885–893, 2017.

[44] Naureen, Sadanand, P. Lohia, D. Dwivedi, and S. Ameen, "A comparative study of quantum dot solar cell with two different ETLs of WS2 and IGZO using SCAPS-1D simulator," *Solar*, vol. 2, no. 3, pp. 341–353, 2022.

[45] T. Minemoto and M. Murata, "Impact of work function of back contact of perovskite solar cells without hole transport material analyzed by device simulation," *Current Applied Physics*, vol. 14, no. 11, pp. 1428–1433, 2014.

[46] F. Baig, Y. H. Khattak, B. Mari, S. Ullah, H. Ullah, and S. Ahmed, "Efficiency enhancement of SnS solar cell using back surface field," in *2018 1st International Conference on Power, Energy and Smart Grid (ICPESG)*, pp. 1–5, Mirpur Azad Kashmir, 2018.

[47] R. Safa Sultana, A. N. Bahar, M. Asaduzzaman, and K. Ahmed, "Numerical modeling of a CdS/CdTe photovoltaic cell based on ZnTe BSF layer with optimum thickness of absorber layer," *Cogent Engineering*, vol. 4, no. 1, 2017.

[48] A. Sunny, S. Rahman, M. M. Khatun, and S. R. Ahmed, "Numerical study of high performance HTL-free CH3NH3SnI3-based perovskite solar cell by SCAPS-1D," *AIP Advances*, vol. 11, no. 6, article 065102, 2021.

[49] D. N. Agha and Q. T. Algwari, "The influence of the interface layer between the electron transport layer and absorber on the performance of perovskite solar cells," *IOP Conference Series: Materials Science and Engineering*, vol. 1152, no. 1, article 012033, 2021.

[50] A. Belghachi and N. Limam, "Effect of the absorber layer bandgap on CIGS solar cell," *Chinese Journal of Physics*, vol. 55, no. 4, pp. 1127–1134, 2017.

[51] X. Zhou and J. Han, "Design and simulation of C2N based solar cell by SCAPS-1D software," *Materials Research Express*, vol. 7, no. 12, article 126303, 2020.